J Mol Model (2013) 19:3931–3939
DOI 10.1007/s00894-013-1933-6

ORIGINAL PAPER

Equilibrium and folding simulations of NS4B H2 in pure water and water/2,2,2-trifluoroethanol mixed solvent: examination of solvation models

Man Guo · Ye Mei

Received: 8 April 2013 / Accepted: 23 June 2013 / Published online: 7 July 2013

Abstract The structural stability and preference of a protein are highly sensitive to the environment accommodating it. In this work, the solvation effect on the structure and folding dynamics of a small peptide, NS4B H2, was studied by computer simulation. The native structure of NS4B H2 was solved previously in 50 % v/v water/2,2,2-trifluoroethanol (TFE) mixed solvent. In this work, both pure water and water/TFE cosolvent were utilized. The force field parameters for water were taken from the TIP3P water model, and those for TFE were generated following the routine of the general AMBER force field (GAFF). The simulated structure of NS4B H2 in the mixed solvent is quite in line with experimental data, while in pure water it undergoes a large structural deformation. The generalized Born (GB) model was also investigated by tuning the dielectric constant to match experimental measurements. However, the results show that its performance was less satisfactory. Two independent direct folding simulations of NS4B H2 in explicit water/TFE cosolvent were carried out, both of which resulted in successful folding. Investigation of the distribution of solvent molecules around the peptide indicates that folding is triggered by the aggregation of TFE on the peptide surface.

Keywords 2,2,2-Trifluoroethanol · Molecular dynamics · Protein folding · Solvent model · Aggregation

M. Guo · Y. Mei (✉)
Center for Laser and Computational Biophysics, State Key Laboratory of Precision Spectroscopy, Department of Physics and Institute of Theoretical and Computational Science, East China Normal University, Shanghai 200062, China
e-mail: ymei@phy.ecnu.edu.cn

Introduction

Solvents play an important role in modulating the stability of secondary structures of proteins and peptides. 2,2,2-Trifluoroethanol (TFE) is well known as one of the most efficient inducers of secondary structure, especially helical structure, in peptides. In the last few decades, the impact of fluorinated solvents on the structure of peptides and proteins has been studied extensively by both experimental [1–4] and computational [5–10] means. Various mechanisms by which TFE promotes the stabilization of particular secondary structure elements have been proposed. The dielectric constant of aqueous TFE solution is much lower than that of pure water under ambient conditions, [4] which weakens hydrophobic interactions but enhances electrostatic interactions such as hydrogen bonds [11, 12]. Therefore, an ordered structure with main chain hydrogen bonds is preferred in TFE. In addition, the aggregation of TFE molecules around the peptide gives rise to a matrix that prevents the intrusion of water molecules to the surface of the peptide [4, 6, 8]. It is well known that water is a competitive hydrogen-bond participator, which may destabilize intra-protein hydrogen bonds. Besides, the helix triggering feature may also arise from the reduced entropy penalty associated with α-helix formation after the association of TFE molecules around the protein surface [13].

An accurate description of the interactions between different components in aqueous solution and that between the protein and solvent is essential for realistic biomolecular modeling. Unfortunately, the great majority of force fields are designed for pure solutions, especially pure water solvent under ambient conditions. Several force field parameters for TFE have been proposed, for example by van Buuren and Berendsen [14, 15], De Loof [16], and Fioroni [17]. Physical

properties calculated from these force fields are in qualitative agreement with experimental measurements. So far, none of the currently available force fields outperforms the others to well describe all the properties of pure liquid TFE and water/TFE mixture. Usually, the choice of the most appropriate force field depends on the major properties of interest. In this work, we developed a new force field for a water/TFE mixture based on the philosophy of the general amber force field (GAFF) [18], and studied its performance in modeling the structure and dynamics of a short peptide in this mixed solvent. GAFF is an indispensable tool in the AMBER community for the modeling of small organic molecules. However, its availability for modeling an organic liquid has not been examined fully. In our previous work [19], a detailed study of the performance of GAFF in modeling pure TFE liquid showed that GAFF was satisfactory for the modeling of TFE liquid, although there was still room for improvement.

Nonstructural protein 4B (NS4B) plays a critical role in the formation of the hepatitis C virus (HCV) replication complex—a relatively poorly characterized 27-kDa integral endoplasmic reticulum (ER) membrane protein [20]. It is predicted to contain a cytosolic N-terminus, two amphipathic helices extending from amino acids (AA) 6 to 29 [21] and AA 42 to 66 [22], a central portion that contains four transmembrane segments [23], and a cytosolic C-terminal part that includes two α-helices (AA 201 to 213 N and AA 228 to 254 [H2])[24]. A partial translocation of the N-terminus of NS4B into the ER lumen has been demonstrated, and this transient topology of NS4B might contribute to the induction of membranous vesicles [22, 25]. In addition, the C-terminal palmitoylation on residues Cys257 and Cys261 [26] is important for the oligomerization, which could contribute to membrane web formation and HCV RNA replication [27]. Here, the peptide studied is H2 in the C-terminal portion of NS4B, which is an amphipathic α-helix extending from Ser227 to Ser254. In the following text, this peptide sequence is re-numbered, starting from 1 for Ser27.

In this work, we compared various solvation models for a 50 % (v/v) water/TFE mixture as solvent through MD simulations of NS4B H2. First, we carried out equilibrium MD simulations of this peptide in explicit 50 % (v/v) water/TFE mixed solvent, and compared with simulations in pure water. Both explicit and implicit generalized Born (GB) solvent models were considered. The peptide structure was well maintained in explicit water/TFE cosolvent. In explicit solvent models, the peptide readily formed an ordered helical conformation in the presence of TFE. However, structural deformation was observed in pure water. This result was consistent with previous studies by other groups [6–8]. With the GB water model, the conformation of this peptide was unstable, which was in good agreement with the result in explicit water. However, it was also unstable in GB water/TFE solvent, with a relative dielectric constant set to 53.0, compared to the result from the simulation in explicit water/TFE cosolvent. Considering that the aggregation of TFE molecules around the peptide leads to a much higher TFE concentration in the vicinity of the peptide than the nominal value of the bulk solution, the actual screening effect experienced by this peptide is not close to the macroscopic measurement. Therefore we also carried out a simulation of this peptide in GB with external relative dielectric constant set to that of pure TFE (27.1). However, the result did not improve too much. Therefore, the subsequent folding simulations were carried out only in an explicit water/TFE mixture. We drew consistent conclusions from two independent trajectories that the peptide folded in an explicit 50 % (v/v) water/TFE mixture and the final structures of both trajectories were in good agreement with its NMR structure [28].

Methods

The parameters of the TFE molecule were generated following the standard procedure of GAFF. The initial structure of TFE was optimized at HF/6-31G** level, and the atomic charges were fitted to the electrostatic potential calculated at B3LYP/cc-pvtz level with restraints applied to avoid a large amplitude of atomic charges [29]. Bonded and van der Waals parameters were determined by atom types. The 50 % (v/v) mixed water/TFE solution was generated by putting 1:4 TFE and water molecules in a periodic box utilizing the LEaP module in AmberTools. A 32 ns molecular dynamics (MD) simulation at 300 K in NPT ensemble was carried out to relax this mixture. The final structure with a density of 1.15 g/cm^3 serves as the building blocks of solvent for dissolving the peptide.

The initial structure of the NS4B H2 peptide in the equilibrium simulations was obtained from Protein Data Bank (entry 2KDR [29]). AMBER03 force field parameters were used for the peptide. For simulations in explicit solvent models, the peptide was placed in a periodic truncated octahedron box of either TIP3P water [30] or a mixture of TFE and water. The minimal distance between the peptide and the water box was 1.2 nm and that between the peptide and the water/TFE box was 1.6 nm. A larger buffer size for water/TFE was necessary, because many TFE molecules were removed automatically when dissolving the peptide. Some water molecules must be removed manually to attain the required TFE:water ratio. Therefore there were some bubbles in the solution initially, and the size of the box would shrink during the simulation under constant pressure. Finally, the mixed solvent contains 4,528 TIP3P water molecules and 1,132 TFE molecules. Two chloride ions were added to neutralize each of the systems. For GB solvent models, the GB solvation model proposed by Onufriev, Bashford and Case [31] was employed. The nonpolar

solvation term was excluded. Nonbonded interactions were fully counted without any truncations. A unit dielectric constant was assigned to the solute interior, while the continuum solvent region was assigned a dielectric constant of 78.5, 53.0 and 27.1 for water, water/TFE mixture and pure TFE respectively [4].

For simulations in explicit solvent models, each system was energy minimized by a steepest descent algorithm for 5,000 steps with strong restraints imposed on the solute and was then subjected to a thorough relaxation without any restraints. The optimized structures were heated up to 300 K in 100 ps in water or 5 ns in water/TFE mixed solvent with weak restraints applied to the peptide, followed by a 300 ns production simulation at NTP ensemble. All simulations were carried out under ambient conditions by employing the Berendsen algorithm [32] to regulate the temperature and pressure with τ_T=0.25 ps and τ_P=2.0 ps. The SHAKE algorithm [33] was utilized to constrain all covalent bonds involving hydrogen atoms, and the integral time step of propagation was 2 fs. The particle mesh Ewald algorithm [34] was utilized for long-range interactions with a 10-Å cutoff in real space. The van der Waals interaction was truncated also at 10 Å. For simulations employing the GB model, the simulation setup was quite similar to that in the explicit water box except that only a single energy minimization procedure was applied, and the production simulation extended only to 100 ns. The folding simulation of the peptide started from a linear structure generated by the LEaP module of AmberTools, and it followed the same procedure and conditions as in the equilibrium simulation of the peptide in an explicit water/TFE mixture, except that the simulations extended to 1 μs each. All simulations were performed using the AMBER 11 package [35].

Results and discussion

Equilibrium simulation analysis

Explicit solvent models

Shown in Fig. 1a–f are snapshots extracted evenly from the trajectory in explicit water with a 50 ns interval. The snapshot with the largest root mean-square deviation (RMSD) from the first model of the NMR structure in the trajectory in water/TFE mixed solvent is also shown for comparison (Fig. 1g). In explicit water, the peptide was not stable and unfolding took place at the N-terminus. At 100 ns, two of seven helical turns became random coil and the remaining five turns were distorted and bore a bent shape. Thereafter, refolding and unfolding can be observed several times, according to the time evolution of RMSD shown in Fig. 2. The peptide underwent considerable deformation with RMSD fluctuating back and forth in large amplitude. Refolding (RMSD<2 Å) was found in the second 25 ns. In the last 25 ns, the mean RMSD was around 7 Å and the largest RMSD reached 9.6 Å. While in 50 % (v/v) water/TFE mixed solvent, the peptide was much more stable. Even for the snapshot with the largest RMSD, only a small distortion occurred to the original straight long helix. In majority of the simulation time in water/TFE mixed solvent, the RMSD was below 2 Å, which was apparently in the folded state. Only in the second 100 ns was the peptide partially unfolded, with RMSD approaching 5 Å. It refolded and stayed in the native structure in the final 100 ns. This result was consistent with experimental results in that only in water/TFE cosolvent could the structure of this peptide be determined.

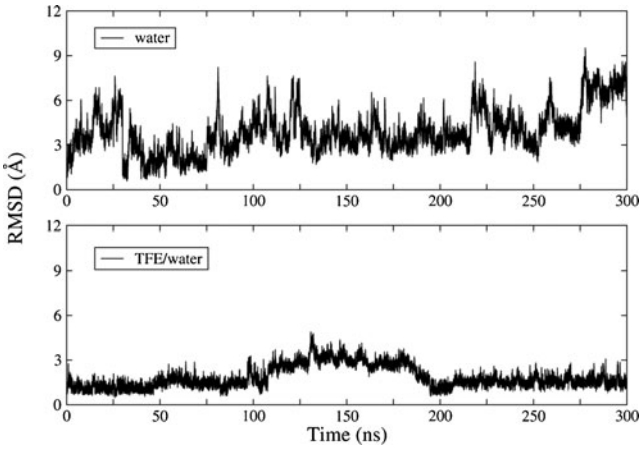

Fig. 2 Backbone RMSD from the first model of NMR structure during equilibrium simulations in (*top*) explicit water and (*bottom*) water/TFE

The unfolding of secondary structure is accompanied by breaking of the main chain hydrogen bonds. We plot in Fig. 3 the variations in bond lengths of the four hydrogen bonds at each end of this peptide. The bond length was measured as

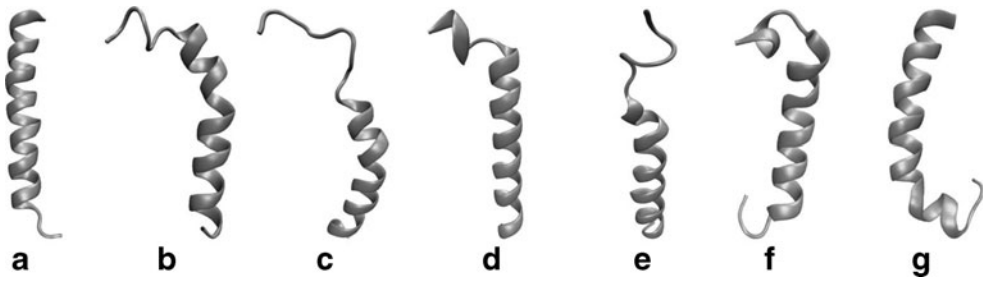

Fig. 1 Snapshots of the peptide taken every 50 ns along the equilibrium trajectory in explicit water (**a**–**f**) and the configuration with maximum root mean-square deviation (RMSD) from the first model of NMR structure in explicit water/2,2,2-trifluoroethanol (TFE) mixture (**g**)

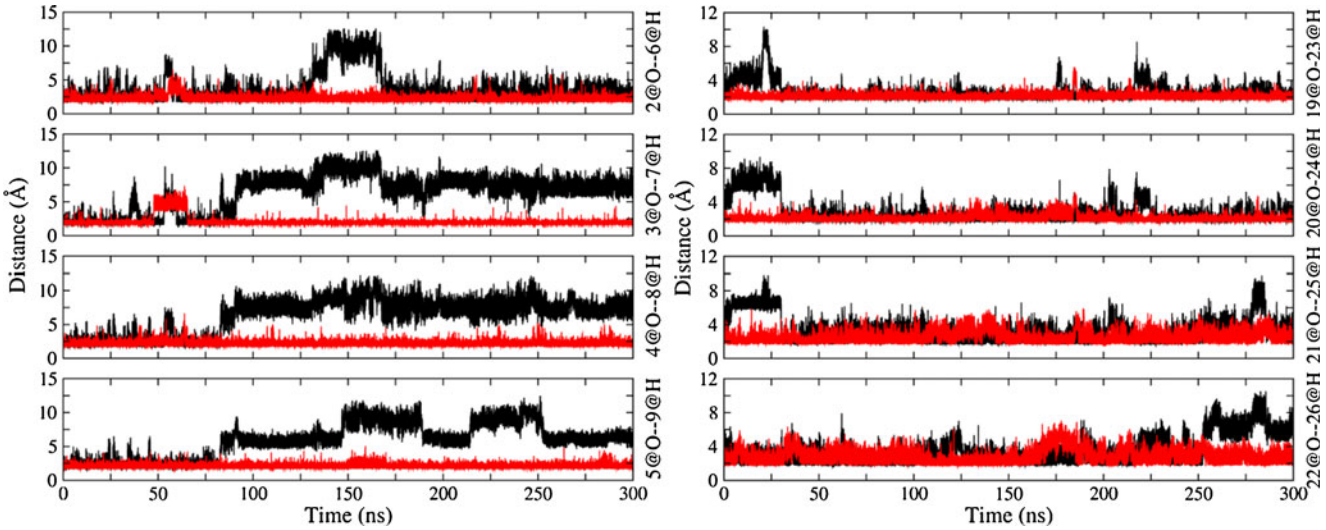

Fig. 3 Variation in hydrogen bond length in the peptide during the equilibrium simulation in explicit water (*black*) and water/TFE (*red*). Atoms are labeled as "residue number@atom name"

the distance between the hydrogen atom involved and the acceptor oxygen atom. When hydrogen-bonded, the distance between these two atoms should be below 2.5 Å. In the first 25 ns of the simulation in pure water, 3 (Leu^{19}–Leu^{23}, Leu^{20}–His^{24} and Arg^{21}–Gln^{25}) of the last four hydrogen bonds were broken, and the distance between oxygen and hydrogen atoms went up to over 4 Å. However, they all refolded back in around 30 ns, and remained very stable in the subsequent simulation time. The last hydrogen bond was very stable for 250 ns, but was broken in the last 50 ns. In general, the last four hydrogen bonds were quite stable and remained bonded for most of the simulation time. Nevertheless, the first four hydrogen bonds were vulnerable. The second to the fourth hydrogen bonds (Ala^3–Val^7, Ala^4–Thr^8, Ala^5–Ala^9) broke at about 80 ns, and never reformed. This was consistent with the observation that the N-terminus of this peptide unfolded. On the contrary, all the hydrogen bonds were very stable during the simulation in water/TFE

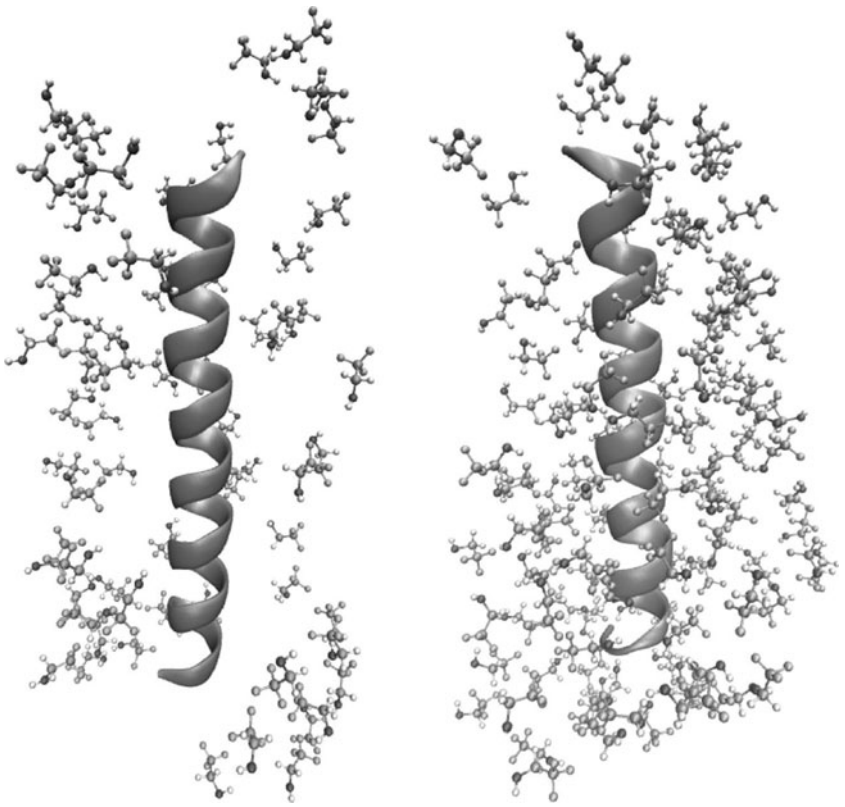

Fig. 4 Comparison of the first and the last snapshots in equilibrium simulation in explicit water/TFE mixed solvent. TFE molecules within 0.6 nm from the peptide are shown

mixed solvent. Only in some minor portion of time was breaking of these hydrogen bonds noted.

Therefore, TFE molecules are essential for the structural stability of this peptide. Understanding the microscopic mechanism of TFE in protecting the helical structure is valuable. In the beginning of the simulation in water/TFE mixed solvent, the water molecules and TFE molecules were distributed evenly around the peptide and in the bulk. With the simulation ongoing, TFE molecules gradually aggregated on the surface of this peptide and pushed water molecules away (see Fig. 4). This phenomenon has also been observed in some other studies [4, 6, 8], and can be explained by the amphipathic nature of TFE. The CF_3 group renders a significant hydrophobicity to the molecule and the electronegativity of fluorine increases the acidity of the hydroxyl group, which makes TFE a better hydrogen bond donor but a poorer hydrogen bond acceptor than a water molecule [36], and allows TFE to reside on the peptide surface. Therefore, the protecting mechanism of water/TFE cosolvent on the helical structure is due not only to the low dielectric constant of this solvent, which may enhance the Coulomb interaction, but also the coating effect of the TFE molecules, which blocks the invasion of water molecules to the main chain hydrogen bonds—the main cause of the destabilization of helical peptide in pure water. The local TFE concentration (LTC) around the peptide residues was calculated by extracting the relative numbers of TFE and water molecules within a 0.6 nm shell surrounding each residue and considering the average excluded volume of 0.019 and 0.07 L/mol for water and TFE, respectively [7, 37]. The LTC for each residue in the system is depicted in Fig. 5. The peak of LTC appears in the center of this peptide, which approaches 0.9. The LTC decays towards both terminals. This is reasonable because the terminal residues are usually more flexible than those in the center of a helix. The high concentration of TFE molecules protects the intra-protein hydrogen bonds from the competition of water molecules in forming hydrogen bonds with the protein. Therefore, the peptide maintains a helical structure.

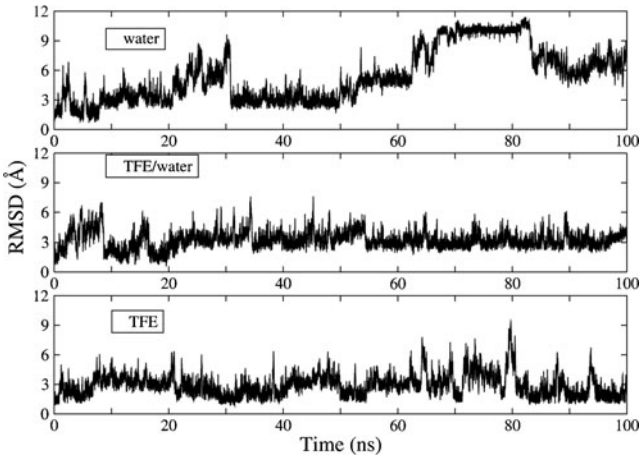

Fig. 6 Backbone RMSDs from the first model of NMR structure along the generalized Born (GB) equilibrium simulations in (*top*) water, (*middle*) water/TFE, and (*bottom*) TFE

GB solvent models

The GB solvent model, as an alternative to the explicit representation of solvent, is particularly attractive because of its algorithmic simplicity and computational efficiency. Unfortunately, the approximations in the GB model also limit its applications in molecular modeling. Therefore it is necessary to study the performance of the GB model in modeling the solvent. The GB solvation model proposed by Onufriev, Bashford and Case [31] as implemented in the AMBER package was employed, with an external relative dielectric constant ε set to 78.5 (water), 53.0 (water/TFE) or 27.1 (pure TFE) [4]. The time series of the backbone RMSDs from the first model of NMR structure in three simulations is shown in Fig. 6. During the simulation in implicit water, the peptide was very flexible, and it quickly unfolded, with

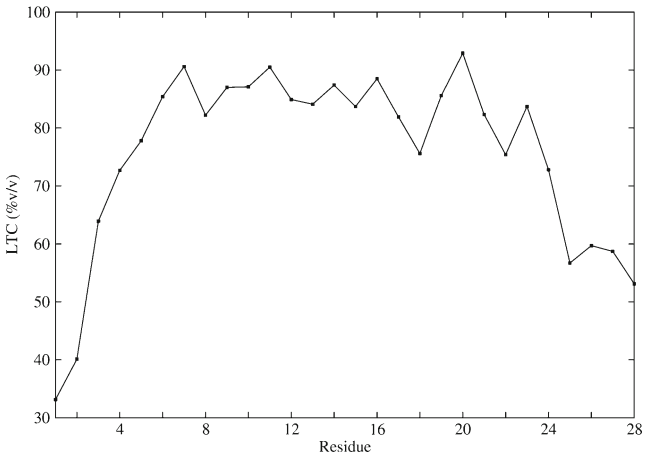

Fig. 5 Average local TFE concentration within a distance of 0.6 nm from the Cα atom of each residue of the peptide in equilibrium simulation

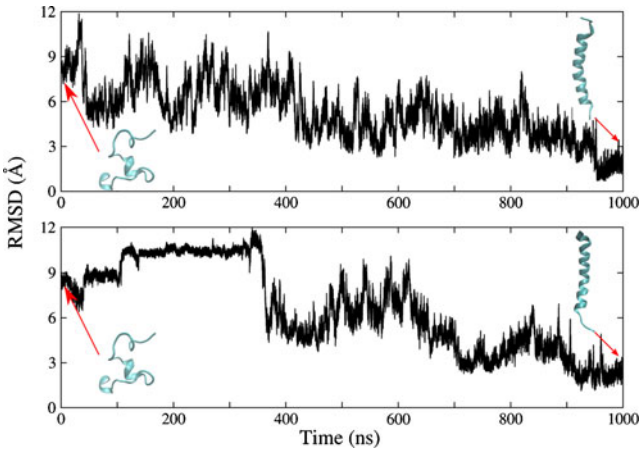

Fig. 7 Backbone RMSDs from the first model of NMR structure in two folding simulations in explicit water/TFE mixture

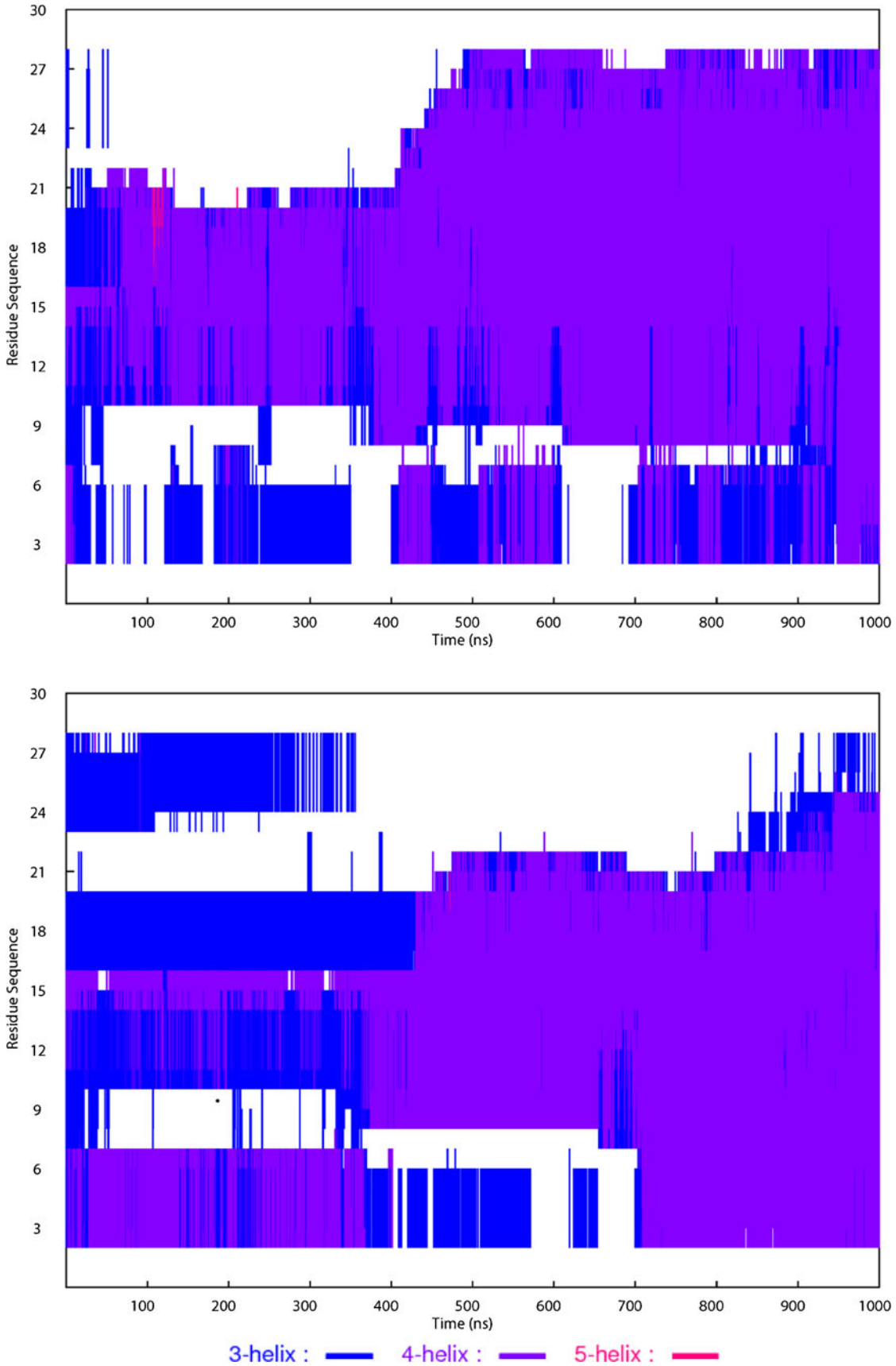

Fig. 8 Variations of the secondary structure in the folding simulations

RMSD approaching 10 Å in 30 ns. Although it also folded back to the native state very quickly, another unfolding event was observed after 50 ns, with RMSD gradually going up to over 10 Å and staying there for 20 ns. This is consistent with the simulation in explicit water, but contrasts with the much suppressed fluctuation of RMSD along the simulation in water/TFE mixed solvent. A discrepancy between simulations in GB and in explicit water/TFE mixture can still be noted. The RMSD fluctuates mainly between 2 and 4 Å, and a larger RMSD over 7 Å can also be seen. It might be argued that the first solvation shell of the peptide in mixed water/TFE is occupied mainly by TFE molecules. Therefore, the dielectric constant is different from the macroscopic measurement. To examine this conjecture, a simulation in implicit solvent with the dielectric constant set to that of pure TFE was also performed. However, the result did not show any improved stability of this peptide over that in ε=53.0. This result shows that an implicit solvent model like GB is not a good model for TFE or water/TFE mixed solvent, and its failure is not due merely to its incapability of representing the inhomogeneous distribution of TFE and water molecules in the first solvent shell and in the bulk.

The discrepancy between explicit solvent model and GB model attributes to the limitations of GB models. The GB model is based on replacing discrete solvent molecules by an infinite continuum with the dielectric properties of the solvent, which is extracted from the fundamental discrete model by several layers of approximations, each of them adding its own limitations on the model. The algorithmic simplicity and computational efficiency, combined with relatively reasonable accuracy of the GB approximation make it attractive in many practical applications of MD simulations of biomolecules, e.g., protein folding and design [38–41], large-scale motions in macromolecules [42–44], peptides and proteins in membrane environments [45–47], and pKa prediction and constant pH simulations [48, 49] etc. However, the GB methodology in modeling more complex environments such as a water/TFE mixture requires a heterogeneous description with a spatially varying dielectric constant. This remains a challenge to the computational biology community. In addition, the dielectric constant changes during the MD simulation with the TFE molecules aggregating around the peptide, which also adds to the difficulty of the GB model.

Folding simulation in explicit water/TFE solvent

Based on the result shown above, the explicit water/TFE mixed solvent model is indispensable to the simulation. Therefore, in the subsequent folding simulations of NS4B H2 in water/TFE cosolvent, the solvent molecules were represented explicitly. Two independent simulations with different initial velocities were carried out, the results of which were quite consistent with only marginal dissimilarities. The RMSDs of backbone atoms from the first model of the NMR structure are shown in Fig. 7. The simulations started with RMSD around 8 Å. It took about 1 μs before folded structures (with RMSD below 2 Å) were seen. This time scale is reasonable for a long helix [50]. The first trajectory (shown as a black line in Fig. 7) showed an approximately three-stage folding processes. Together with the dictionary of secondary structure of proteins (DSSP) [51] analysis (see the top panel in Fig. 8), we found that two helices (residues 3–6 and 10–20) formed very quickly and remained very stable and unmerged in the first 400 ns. The short helix was mainly a 3_{10} helix. The long helix grew towards the C-terminus, and elongated by eight residues in the next 100 ns. This structure held for about 400 ns. Finally, in the last 100 ns, these two helices merged together and the RMSD dropped to below 2 Å. Another trajectory showed only some trivial differences. In the very beginning of this simulation, three helices (residues 3–7, 10–20, 23–28) formed quickly. The helix close to the N-terminus is an α-helix, while the other two are 3_{10} helices. The helix close to the C-terminus (residues 23–28) unfolded at 370 ns, and remained as a random coil in the next 500 ns. At the same time, the central helix switched to an α-helix, while the first helix changed into an 3_{10} helix. At 700 ns, these two helices merged together, and extended towards the C-terminus. The folded structure was arrived at after 900 ns.

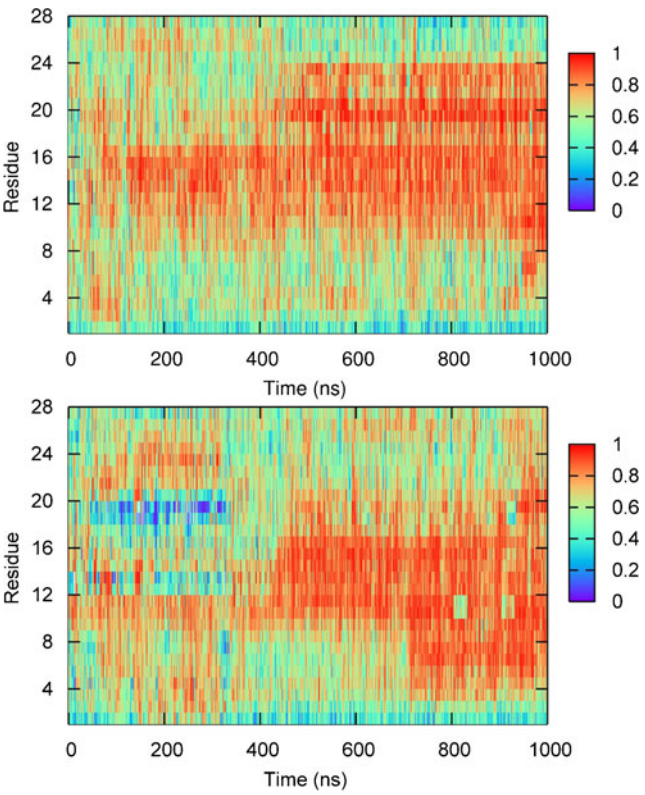

Fig. 9 Variations of local TFE concentration (LTC) in the folding simulations

The variation of the LTC around the peptide is shown in Fig. 9. At the beginnings of both simulations, the LTC was around 50 %, but it gradually increased during the simulations. We noticed that the increase in LTC and the formation of helical residues were highly correlated. In the final stage of these simulations, the LTC approached 100 % for the central residues, and decayed toward two terminals. This result was consistent with the equilibrium MD simulation. This observation serves as direct evidence that TFE is an effective inducer of helix.

Conclusions

In this work, both equilibrium and folding simulations were carried out to study the solvation effect of TFE on the structure of a small peptide. The structure of this peptide, which is a long helix, was solved in 50 % (v/v) TFE. In equilibrium simulations, both explicit and implicit solvation models have been utilized and compared. Explicit solvent models provide arguably the most accurate description of the solvation effect. The potential function of TFE was produced following the routine of the general AMBER force field. The peptide is partly unfolded in water but adopts an ordered helical conformation in a water/TFE mixture, which is in agreement with the experimental observations [28]. Furthermore, the accumulation of TFE molecules in the immediate vicinity of this peptide was observed, which prevents the formation of alternative hydrogen bonds between water and the peptide. Besides, it provides a low dielectric environment that stabilizes the main chain hydrogen bonds in the peptide.

The folding simulations were performed in explicit water/TFE solvent. These two trajectories show only trivial differences. The folding takes place mainly from central residues, and elongates towards the terminals. The helical segments merge together in the final stage. DSSP and LTC analysis of the trajectories shows that the folding is accompanied by the aggregation of TFE molecules on the peptide surface. This coating effect promotes the formation of local interactions and, as a consequence, an ordered secondary structure. This observation is consistent with the experimental understanding that TFE is an effective trigger of secondary structure, especially of helical conformation.

These simulations have demonstrated the effectiveness of this water/TFE mixed solvent model. However, GB representation of the water/TFE mixed solvent failed to obtain results in agreement with the explicit solvent model. Although GB methodology is successful in modeling simple homogeneous and invariable dielectric environment [46, 52, 53], the water/TFE mixed solvent is more complex and requires a heterogeneous and alterable description of dielectric constant in order to depict the aggregated TFE molecules. So the GB solvent model is not an appropriate choice for water/TFE mixture so far.

Acknowledgments This work is supported by the National Natural Science Foundation of China (Grant No. 21173082) and the Shanghai Rising-Star Program (Grant No. 11QA1402000). We thank Supercomputer Center of East China Normal University for CPU time support.

References

1. Harris KR, Newitt PJ, Derlacki ZJ (1998) Alcohol tracer diffusion, density, NMR and FTIR studies of aqueous ethanol and 2,2,2-trifluoroethanol solutions at 25°C. J Chem Soc Faraday Trans 94:1963–1970
2. Jasanoff A, Fersht AR (1994) Quantitative determination of helical propensities from trifluoroethanol titration curves. Biochemistry 33:2129–2135
3. Buck M (1998) Trifluoroethanol and colleagues: cosolvents come of age. Recent studies with peptides and proteins. Q Rev Biophys 31:297–355
4. Hong DP, Hoshino M, Kuboi R, Goto Y (1999) Clustering of fluorine-substituted alcohols as a factor responsible for their marked effects on proteins and peptides. J Am Chem Soc 121:8427–8433
5. Rezaei-Ghaleh N, Amininasab M, Nemat-Gorgani M (2008) Conformational changes of α-chymotrypsin in a fibrillation-promoting condition: a molecular dynamics study. Biophys J 95:4139–4147
6. Mehrnejad F, Naderi-Manesh H, Ranjbar B (2007) The structural properties of magainin in water, TFE/water, and aqueous urea solutions: molecular dynamics simulations. Proteins Struct Funct Bioinform 67:931–940
7. Mehrnejad F, Chaparzadeh N (2008) Structural and dynamical studies of Humanin in water and TFE/water mixture: a molecular dynamics simulation. J Biomol Struct Dyn 26:255–262
8. Roccatano D, Colombo G, Fioroni M, Mark AE (2002) Mechanism by which 2,2,2-trifluoroethanol/water mixtures stabilize secondary-structure formation in peptides: a molecular dynamics study. Proc Natl Acad Sci USA 99:12179–12184
9. Roccatano D, Fioroni M, Zacharias M, Colombo G (2005) Effect of hexafluoroisopropanol alcohol on the structure of melittin: A molecular dynamics simulation study. Protein Sci 14:2582–2589
10. Fioroni M, Diaz MD, Burger K, Berger S (2002) Solvation phenomena of a tetrapeptide in water/trifluoroethanol and water/ethanol mixtures: a diffusion NMR, intermolecular NOE, and molecular dynamics study. J Am Chem Soc 124:7737–7744
11. Uversky VN, Narizhneva NV, Kirschstein SO, Winter S, Löber G (1997) Conformational transitions provoked by organic solvents in β-lactoglobulin: can a molten globule like intermediate be induced by the decrease in dielectric constant? Fold Des 2:163–172
12. Rajan R, Balaram P (1996) A model for the interaction of trifluoroethanol with peptides and proteins. Int J Pept Protein Res 48:328–336
13. Aurora R, Creamer TP, Srinivasan R, Rose GD (1997) Local interactions in protein folding: lessons from the α-helix. J Biol Chem 272:1413–1416
14. van Buuren AR, Berendsen HJC (1993) Molecular dynamics simulation of the stability of a 22-residue α-helix in water and 30% trifluoroethanol. Biopolymers 33:1159–1166
15. Chitra R, Smith PE (2001) Properties of 2,2,2-trifluoroethallol and water mixtures. J Chem Phys 114:426–435
16. Deloof H, Nilsson L, Rigler R (1992) Molecular dynamics simulation of galanin in aqueous and nonaqueous solution. J Am Chem Soc 114:4028–4035
17. Fioroni M, Burger K, Mark AE, Roccatano D (2000) A new 2,2,2-trifluoroethanol model for molecular dynamics simulations. J Phys Chem B 104:12347–12354

18. Wang JM, Wolf RM, Caldwell JW, Kollman PA, Case DA (2004) Development and testing of a general amber force field. J Comput Chem 25:1157–1174
19. Jia XY, Zhang JZH, Mei Y (2013) Assessing the accuracy of the general AMBER force field for 2,2,2-trifluoroethanol as solvent. J Mol Model 19:2355–2361. doi: 10.1007/s00894-013-1776-1
20. Huegle T, Fehrmann F, Bieck E, Kohara M, Kraeusslich H-G, Rice CM et al (2001) The hepatitis C virus nonstructural protein 4B is an integral endoplasmic reticulum membrane protein. Virology 284:70–81
21. Elazar M, Liu P, Rice CM, Glenn JS (2004) An n-terminal amphipathic helix in hepatitis C virus (HCV) NS4B mediates membrane association, correct localization of replication complex proteins, and HCV RNA replication. J Virol 78:11393–11400
22. Gouttenoire J, Castet V, Montserret R, Arora N, Raussens V, Ruysschaert J-M et al (2009) Identification of a novel determinant for membrane association in hepatitis C virus nonstructural protein 4B. J Virol 83:6257–6268
23. Lundin M, Monne M, Widell A, von Heijne G, Persson MAA (2003) Topology of the membrane-associated hepatitis C virus protein NS4B. J Virol 77:5428–5438
24. Gouttenoire J, Penin F, Moradpour D (2010) Hepatitis C virus nonstructural protein 4B a journey into unexplored territory. Rev Med Virol 20:117–129
25. Lundin M, Lindstrom H, Gronwall C, Persson MAA (2006) Dual topology of the processed hepatitis C virus protein NS4B is influenced by the NS5A protein. J Gen Virol 87:3263–3272
26. Yu GY, Lee KJ, Gao L, Lai MMC (2006) Palmitoylation and polymerization of hepatitis C virus NS4B protein. J Virol 80:6013–6023
27. Gouttenoire J, Roingeard P, Penin F, Moradpour D (2010) Amphipathic alpha-helix AH2 Is a major determinant for the oligomerization of hepatitis C virus nonstructural protein 4B. J Virol 84:12529–12537
28. Gouttenoire J, Montserret R, Kennel A, Penin F, Moradpour D (2009) An amphipathic alpha-helix at the C terminus of hepatitis C virus nonstructural protein 4B mediates membrane association. J Virol 83:11378–11384
29. Bayly CI, Cieplak P, Cornell WD, Kollman PA (1993) A well-behaved electrostatic potential based method using charge restraints for deriving atomic charges: the RESP model. J Phys Chem 97:10269–10280
30. Jorgensen WL, Chandrasekhar J, Madura JD, Impey RW, Klein ML (1983) Comparison of simple potential functions for simulating liquid water. J Chem Phys 79:926–935
31. Onufriev A, Bashford D, Case DA (2004) Exploring protein native states and large-scale conformational changes with a modified generalized born model. Proteins Struct Funct Bioinform 55:383–394
32. Berendsen HJC, Postma JPM, Vangunsteren WF, Dinola A, Haak JR (1984) Molecular dynamics with coupling to an external bath. J Chem Phys 81:3684–3690
33. Ryckaert JP, Ciccotti G, Berendsen HJC (1977) Numerical integration of the Cartesian equations of motion of a system with constraints: molecular dynamics of n-alkanes. J Comput Phys 23:327–341
34. Darden T, York D, Pedersen L (1993) Particle mesh Ewald: An N·log(N) method for Ewald sums in large systems. J Chem Phys 98:10089–10092
35. Case DA, Darden TA, Cheatham TE III, Simmerling CL, Wang J et al (2010) Amber 11. University of California, San Francisco Estuary and Watershed Science
36. Llinás M, Klein MP (1975) Charge relay at the peptide bond. Proton magnetic resonance study of solvation effects on the amide electron density distribution. J Am Chem Soc 97:4731–4737
37. Marcus Y (1998) Wiley series in solution chemistry. The properties of solvents. Wiley, Chichester, NY
38. Zagrovic B, Snow CD, Shirts MR, Pande VS (2002) Simulation of folding of a small alpha-helical protein in atomistic detail using worldwide-distributed computing. J Mol Biol 323:927–937
39. Simmerling C, Strockbine B, Roitberg AE (2002) All-atom structure prediction and folding simulations of a stable protein. J Am Chem Soc 124:11258–11259
40. Lei H, Duan Y (2007) Ab initio folding of albumin binding domain from all-atom molecular dynamics simulation. J Phys Chem B 111:5458–5463
41. Lopes A, Alexandrov A, Bathelt C, Archontis G, Simonson T (2007) Computational sidechain placement and protein mutagenesis with implicit solvent models. Proteins Struct Funct Bioinform 67:853–867
42. Tsui V, Case DA (2000) Theory and applications of the Generalized Born solvation model in macromolecular simulations. Biopolymers 56:275–291
43. Amaro RE, Cheng X, Ivanov I, Xu D, McCammon JA (2009) Characterizing loop dynamics and ligand recognition in human- and avian-type influenza neuraminidases via generalized Born molecular dynamics and end-point free energy calculations. J Am Chem Soc 131:4702–4709
44. Chocholousova J, Feig M (2006) Implicit solvent simulations of DNA and DNA-protein complexes: Agreement with explicit solvent vs experiment. J Phys Chem B 110:17240–17251
45. Spassov VZ, Yan L, Szalma S (2002) Introducing an implicit membrane in generalized Born/solvent accessibility continuum solvent models. J Phys Chem B 106:8726–8738
46. Tanizaki S, Feig M (2005) A generalized Born formalism for heterogeneous dielectric environments: application to the implicit modeling of biological membranes. J Chem Phys 122:124706-1-13
47. Ulmschneider MB, Ulmschneider JP, Sansom MSP, Di Nola A (2007) A generalized Born implicit-membrane representation compared to experimental insertion free energies. Biophys J 92:2338–2349
48. Spassov VZ, Yan L (2008) A fast and accurate computational approach to protein ionization. Protein Sci 17:1955–1970
49. Mongan J, Case DA, McCammon JA (2004) Constant pH molecular dynamics in generalized born implicit solvent. J Comput Chem 25:2038–2048
50. Kubelka J, Hofrichter J, Eaton WA (2004) The protein folding 'speed limit'. Curr Opin Struct Biol 14:76–88
51. Kabsch W, Sander C (1983) Dictionary of protein secondary structure: pattern recognition of hydrogen-bonded and geometrical features. Biopolymers 22:2577–2637
52. Tanizaki S, Clifford J, Connelly BD, Feig M (2008) Conformational sampling of peptides in cellular environments. Biophys J 94:747–759
53. Scarsi M, Apostolakis J, Caflisch A (1998) Comparison of a GB solvation model with explicit solvent simulations: Potentials of mean force and conformational preferences of alanine dipeptide and 1,2-dichloroethane. J Phys Chem B 102:3637–3641